GEOPHYSICAL RESEARCH LETTERS, VOL. 17, NO 11, PAGES 1905 1908, OCTOBER 1990

SIMULTANEOUS, IN SITU MEASUREMENTS OF OH AND HO_2 IN THE STRATOSPHERE

R. M. Stimpfle, P. O. Wennberg, L. B. Lapson and J. G. Anderson

Department of Earth and Planetary Sciences and Department of Chemistry
Harvard University, Cambridge, MA 02138

Abstract. Stratospheric OH and HO_2 radical densities have been measured between 36 and 23 km using a balloon-borne, in situ instrument launched from Palestine, TX on August 25, 1989. OH is detected using the laser-induced fluorescence technique (LIF) employing a Cu-vapor-laser pumped dye laser coupled with an enclosed-flow detection chamber. HO_2 is detected nearly simultaneously by adding NO to the sample flow to convert ambient HO_2 to OH. Observed OH and HO_2 densities ranged from $8.0 \pm 2.8 \times 10^6$ and $1.4 \pm 0.5 \times 10^7$ molec cm^{-3}, respectively, at 36 km, to $1.4 \pm 0.5 \times 10^6$ and $3.0 \pm 1.0 \times 10^6$ at 23 km, where the uncertainty is $\pm 1\sigma$. The HO_2 density exhibits a maximum in the 34-30 km region of $1.7 \pm 0.6 \times 10^7$. The data were obtained over a solar zenith angle variation of 51° at 36 km to 61° at 23 km. O_3 and H_2O densities also were measured simultaneously with separate instruments.

Introduction

The HO_x family of reactants is dominated by the OH and HO_2 species in the stratosphere. The photochemical reactions that control HO_x and the role of HO_x species in the production and loss of stratospheric ozone are critical to predictions of temporal trends in ozone column abundances (see for example WMO [1986]). In the upper stratosphere, OH and HO_2 engage in odd-oxygen recombination by direct reaction with O_3 and O. In the middle and lower stratosphere, OH and HO_2 affect O_x indirectly, through their interaction with the NO_x and Cl_x families of reactants. The response of OH to increasing Cl_x, methane and NO_x in the atmosphere is crucial in determining the effect of these compounds on stratospheric ozone.

A rudimentary method of testing stratospheric HO_x photochemistry has been by direct comparison of individually measured OH and HO_2 densities (and H_2O_2 because it is a key indicator of HO_2) with model calculations. In such comparisons, HO_2 measurements have shown the most striking disparity between measurement and theory. The pioneering measurements of stratospheric HO_2 by cyrogenic matrix sampling, followed by ground-based laboratory ESR detection [Mihelcic et al., 1978; Helten et al., 1984], are higher by an order of magnitude or more than model predictions. An in situ technique based upon OH resonance lamp-induced fluorescence detection of OH formed from the conversion of HO_2 to OH by NO addition [Anderson et al., 1981] gave results in better agreement with model predictions but still larger than expected. A ground based, mm-wave spectroscopy, column HO_2 measurement [de Zafra et al., 1984] that is most sensitive to density variations in the 38–65 km interval did not support the HO_2 densities reported below 37 km by the aforementioned investigators. The disagreement among these HO_2 measurements led to questions concerning the validity of each measurement. The discrepancy between model calculations and the measurements below 38 km, if they are indeed valid, would imply serious errors in our understanding of stratospheric photochemistry, such as missing photochemical mechanisms.

The most recently published HO_2 measurement uses a far-infrared spectrometer to observe thermal emission in a limb scanning mode from a balloon-borne gondola in the 49–23 km interval [Traub et al., 1990]. This measurement agrees with the column measurement of deZafra et al. [1984], leading to an HO_2 altitude profile from these two measurements in good agreement (within a factor of two) with theoretical models. In this paper we present new, high signal-to-noise, in situ HO_2 measurements in the 37-23 km interval that agree with the conclusions drawn by Traub et al. [1990] that HO_2 densities are not in profound disagreement with current models.

The instrument used here is based upon an OH detection technique. HO_2 is detected as above [Anderson et al., 1981] by adding NO to the atmospheric sample to convert HO_2 to OH. Nearly simultaneous measurements of the OH radical density are acquired during times when no NO is injected into the flow. The main body of balloon-borne OH measurements (see Stimpfle et al. [1989]) displays less scatter than the HO_2 data base and can be considered to be in broad agreement with model predictions. The new OH measurements reported here do not change that conclusion. However, by detecting OH and HO_2 simultaneously, the leverage provided by this technique to test HO_x photochemical mechanisms used in model calculations is greatly enhanced. The measured ratio of HO_2 to OH provides a direct, in situ test of the small subset of reactions that control the rapid cycling of HO_x radicals between the OH and HO_2 species. Additionally, the uncertainty in the ratio is less than that of the individual OH and HO_2 measurements, because error in the absolute OH detection sensitivity cancels out.

In this paper we discuss the experimental modifications made in preparation for the flight described here and present the results of the flight.

Experimental

The OH detection instrument uses the LIF technique and has been described previously [Stimpfle et al., 1989; Stimpfle and Anderson, 1988]. OH is optically pumped in the A-X (1,0) band via the $Q_1(1)$ line at 282 nm with a 17-kHz repetition rate, Cu-vapor-laser pumped dye laser. OH A-X, (0,0) band fluorescence centered at 309 nm is observed with a filtered photomultiplier tube. Detection takes place in the core of a flowing sample of ambient

Paper number 90GL01825
0094-8276/90/90GL-01825$03.00

stratospheric air as it is drawn through a cylindrical detection chamber during controlled balloon descent from peak altitude. The OH fluorescence signal, S^{OH}, is distinguished from the background signal by successively step tuning the laser on and off resonance with the OH absorption line in equal 10-s increments.

Two significant modifications have been made to the instrument in preparation for the flight reported here:

First, the ability to detect HO_2 in addition to OH was included by adding an NO gas addition subsystem to the detection pod. The

$$HO_2 + NO \rightarrow OH + NO_2 \qquad (1)$$

reaction converts ambient HO_2 to OH in the presence of excess NO. The NO is added to the sample flow through a circular array of 32, black teflon coated, 0.16 cm o.d., stainless steel tubes. The fixture is located 40.5 cm upstream of the fluorescence detection volume at a 12.7-cm i.d. section of the flow tube. This position typically allows 15 ms of reaction time at the flow velocities achieved in flight.

Second, the absolute OH detection sensitivity was increased by a factor of ~12 by adopting a new optical design for the fluorescence detection axis. In previous flights of this instrument (July 15, 1987 and July 6, 1988) the detector consisted of a fiber optic cable coupled to the curved entrance slit of a 1/4 m spectrometer. A PMT at the exit slit detected OH fluorescence. In order to increase the absolute OH detection sensitivity, the photomultiplier tube was relocated to the detection pod with a front-end optical system employing two optical elements. The first is a sealed quartz cell, 1-mm inner wall spacing, containing a solution of potassium hydrogen pthalate dissolved in methyl alcohol. This liquid, UV cut-off filter effectively absorbs Rayleigh ($T \leq 1 \times 10^{-6}$ at 282 nm) and N_2 Raman ($T \sim 5 \times 10^{-2}$ at 302 nm) scattered laser light while preserving a high transmission for OH fluorescence (T = 0.8 at 309 nm). The second optical element is a 1.5-in diameter interference filter, with peak T = 0.22 at 310 nm and a FWHM band pass of 4 nm. The optical elements are housed in a thermostated aluminum block to prevent temperature induced drifts of the interference filter pass band and transmission.

The instrument was calibrated before flight in the manner described previously [Stimpfle et al., 1989]. The observed count rate due to OH, S^{OH} (counts s^{-1}), is given by the following expression:

$$S^{OH} = C^{OH} E Q [OH]$$

where C^{OH} is the calibration constant determined by direct measurement, E is the power (mW), Q is the fluorescence efficiency (unitless), and [OH] is the density (molec cm^{-3}). The instrumental sensitivity was found to be:

$$C^{OH} = 1.4 \pm 0.5 \times 10^{-4} \left(\frac{\text{counts/s}}{\text{mW} \cdot Q \cdot [OH]} \right)$$

The flight NO injector head was tested in the flow bench and found to produce no observable losses of OH. The HO_2 conversion was tested qualitatively by checking that the selected NO mass flow rates were adequate for driving reaction (1) to completion in the time scale allowed. The NO addition cycle is described below.

Results and Discussion

The experiment was launched at 1602 UT (1023 CDT) on August 25, 1989 from the National Scientific Balloon Facility in Palestine, TX. A float altitude of 37.9 km was attained at approximately 1820 UT. The controlled descent period of the flight was initiated in the afternoon at 2202 UT, 51° solar zenith angle (SZA), and terminated at 2248 UT, 61° SZA, at an altitude of 23.1 km. The unexpectedly long period of time before descent was required by safety considerations concerning the location of the ground track defined by the balloon trajectory.

The instrument operated flawlessly during the 46 min descent period with excellent signal-to-noise. A 160-s segment of unaveraged (1/4 s), 309 nm detector data in the 31.5–30.7 km interval is shown in the top panel of Figure 1. The NO addition and laser tuning cycles are also displayed to illustrate their synchronization with the signal. The laser is tuned on and off resonance with the $Q_1(1)$ OH absorption line in the 20-s cycle shown in the lower panel of Figure 1. The NO addition cycle (middle panel) consists of two different, successively alternating, NO flow rates. The NO addition starts at the beginning of an off-resonant measurement to check for NO effects on the background. At the end of the following on-resonant measurement, the NO flow is terminated and immediately followed by a 4-s N_2 purge. The purge flushes NO out of the injector prior to the next on-resonant measurement, corresponding to an ambient OH measurement where there is no gas addition. NO addition is then repeated as above with a second NO flow, a factor of 0.4 that of the first. A complete 80-s cycle consists of four alternating OH and HO_2 measurements, with the HO_2 measurements made with two different NO flow rates. With a gondola descent velocity of ~ 5 m s^{-1}, each radical measurement is completed within a vertical distance of 100 m.

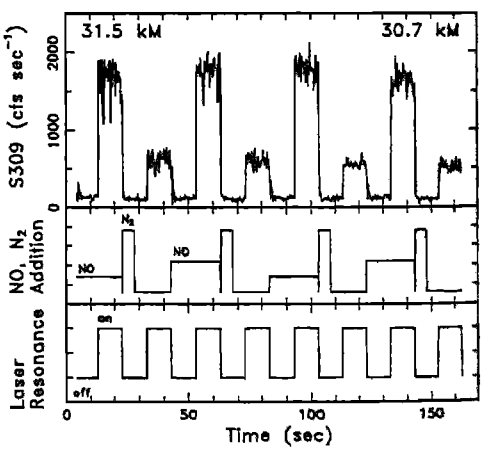

Fig. 1. Unaveraged 309 nm detector count rate data (top), NO and N_2 gas addition sequence (middle), and laser tuning cycle (lower) vs. time, during balloon descent through the 31.5–30.7 km interval.

The signal observed in the presence of NO is due to both ambient OH and that produced by NO reaction with HO_2. Extracting HO_2 densities from the count rate data

is slightly complicated by the three-body reaction of OH with NO:

$$OH + NO + M \rightarrow HONO + M \qquad (2)$$

This reaction is slow at 37 km, but becomes increasingly important as air density increases. For this reason two different NO flow rates are used as a simple test to check completeness of the conversion reaction. The relative invariance of the observed signal to the two NO flow rates over a large dynamic range in pressure is evidence that the conversion was essentially optimal, i.e., in a region near peak conversion. Altitude dependent values for the fraction of ambient OH surviving recombination with NO (c_1) and the fractional conversion of HO_2 to OH (c_2) are calculated from the known temperature-dependent rate constants for (1) and (2) [DeMore et al., 1988], and the observed temperature and pressure. c_1 decreases from 0.93 to 0.73 between 37 and 23 km, and c_2 decreases from 0.92 to 0.70. Using these values, the HO_2 density is given by the following expression:

$$[HO_2] = \left([OH]^{NO\ on} - \left([OH]^{NO\ off} \times c_1\right)\right) \times 1/c_2$$

where $[OH]^{NO\ on}$ is the observed OH in the presence of NO, and $[OH]^{NO\ off}$ is the average, observed ambient [OH] bracketting $[OH]^{NO\ on}$. If we are not optimally converting HO_2 to OH we will systematically underestimate $[HO_2]$ by this method.

The observed OH and HO_2 profiles are shown in Figure 2. Each point is the result of a 20-s integration period, yielding a vertical resolution of ~ 100 m. Two HO_2 profiles are shown corresponding to the results obtained with each NO flow rate. There is an indication that the lower NO flow has slightly less conversion throughout the descent but the difference is not significant in comparison with the estimated uncertainity in the overall accuracy of ±35% for [OH] given by uncertainities in the calibration and the fluorescence efficiency. The uncertainity in $[HO_2]$ is slightly greater, ±38%, due mainly to uncertainity orginating in the rate constant for (2). The increased OH sensitivity has greatly reduced imprecision due to counting statistics in comparison with previous flights. The shot-noise contribution ranges from ±0.7% at 36 km to ±20% at 23 km.

The observed fine structure in the OH and HO_2 profiles shown in Figure 2 cannot be considered real until we have eliminated possible instrumental effects as a cause. Photochemical mechanisms do not provide a clue concerning the authenticity of the observed structure in this case, because there is no significant covariance of OH and HO_2. The observed scatter may simply represent our current instrumental precision, limited by our ability to account for frequency or power fluctuations, or small perturbations to the flow that are not indicated by the flow temperature measurement.

The HO_2 results, expressed in mixing ratio, are compared with previous HO_2 measurements in Figure 3. This figure is taken from the summary of Traub et al. [1990] in which the results of Helten et al. [1984] and Anderson et al. [1981] are scaled to matching SZA of 54° corresponding to the Traub FTIR measurement. Our results, measured between 51° and 61° SZA, need not be scaled

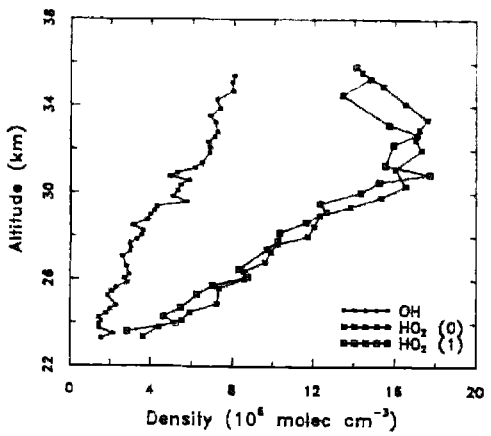

Fig. 2. [OH] and $[HO_2]$ vs. altitude observed Aug. 25, 1989, over a solar zenith angle variation of 51°-61°. HO_2 (0) and (1) refer to high and low NO flow rate results, respectively.

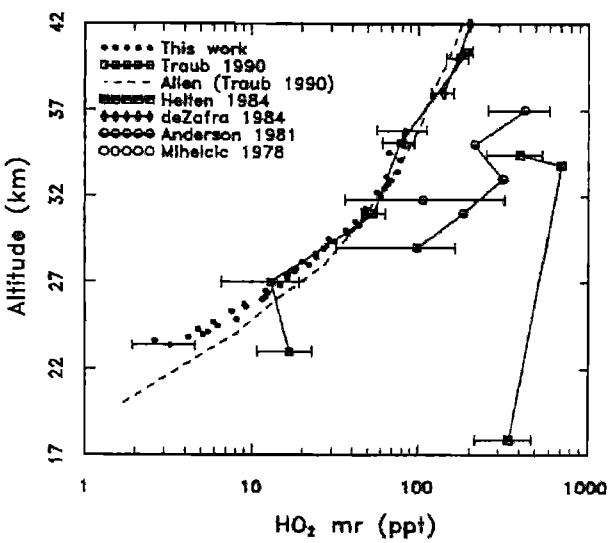

Fig. 3. Summary of HO_2 mixing ratio measurements vs. altitude from Traub et al. [1990], at 54° solar zenith angle. Measurements by Traub et al. [1990], Anderson et al. [1981], de Zafra et al. [1984], Helten et al. [1984], and model calculation by M. A. Allen (from Traub et al. [1990]). Amended to include results from Mihelcic et al. [1978] and this work.

for a meaningful comparison. As can be seen in Figure 3, this data set is in good agreement with the results of Traub et al. [1990] and therefore with the extrapolated profile of deZafra et al. [1984]. Convergence of HO_2 measurements obtained by three different techniques provides strong evidence that HO_2 has been validly measured in the stratosphere. Our HO_2 measurements will be repeated to further diagnose details of the NO conversion kinetics by modifying the gas addition scheme to include three NO flow rates in more rapid sequential addition.

The present OH results are compared with previous OH measurements made with this instrument in Figure 4. Since the earlier flights were characterised by relatively low SZA, 14°-9° [Stimpfle and Anderson, 1988] and 15°

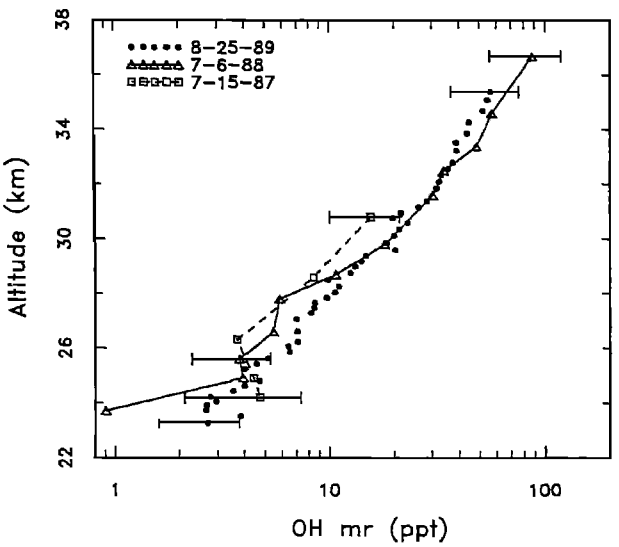

Fig. 4. Comparison of OH mixing ratio measurements vs. altitude made with this instrument, from Stimpfle and Anderson [1988], Stimpfle et al. [1989], and this work.

27° [Stimpfle et al., 1989], the present measurements have been scaled to ~ 24° to remove the SZA difference using typical, mid-latitude photochemical model results (S. Lloyd, private communication). The correction is a multiplicative factor ranging from 1.2 at 36 km to 2.0 at 23 km. The agreement among the three data sets is good if the simple standard of overlapping error bars ($\pm 1\sigma$), which combine the precision and the estimated error in the absolute accuracy, is taken as the criterion. The most significant variation is the different shape of the July 6, 1988 and August 25, 1989 profiles in the 26–29 km region. Differences of this quality may simply represent year-to-year variation of dynamic and photochemical variables that control HO_x source and sink species. Our simultaneous measurements of O_3 and H_2O indicate that variation of these species is not responsible for the variation of the OH profiles in Figure 4. Variation of other parameters that can affect HO_x species limits the level of detail to which comparisons of HO_x data from different air masses can be carried out.

The major advance given by the data described here is that we are now able to examine two critical elements of HO_x photochemistry with a data set from the same air mass. First, we can examine the ratio of HO_2 to OH that is believed to be controlled principally by NO, O_3 and O. This partitioning is critical in determining the interaction of HO_x with the NO_x and Cl_x species in the stratosphere. Secondly, we can begin an examination of HO_x production and loss balance. Production is proportional to $[O_3]$ and H_2O mixing ratio throughout the stratosphere. Loss is proportional to the product of [OH] and $[HO_2]$ above 30 km and becomes dominated by reactions of OH with NO_y species in the lower stratosphere. An examination of these issues is presented in a separate paper [Wennberg et al., 1990].

Acknowledgments This flight could not have been carried out without the special assistance on short notice of a large number of individuals: At NASA headquarters, Bob Watson; at NSBF, Danny Ball and the NSBF support staff, which provided excellent assistance; and at Harvard, E. Weinstock, J. Demusz, N. Hazen, B. Heroux, T. Schiller, D. Spillane and E. Thompson. Funds provided by NASA contract NASW 3960.

References

Anderson, J. G., H. J. Grassl, R. E. Shetter, and J. J. Margitan, HO_2 in the stratosphere: Three in-situ observations, *Geophys. Res. Lett.*, *8*, 289–292, 1981.

de Zafra, R. L., A. Parrish, P. M. Solomon, and J. W. Barrett, A measurement of stratospheric HO_2 by ground-based millimeter-wave spectroscopy, *J. Geophys. Res.*, *89*, 1321–1326, 1984.

DeMore, W. B., M. J. Molina, S. P. Sander, D. M. Golden, R. F. Hampson, M. J. Kurylo, C. J. Howard, and A. R. Ravishankara, NASA Public. 87-41, 1988.

Helten, M., W. Patz, M. Trainer, H. Fark, E. Klein, and D. H. Ehhalt, Measurements of stratospheric HO_2 and NO_2 by matrix isolation and ESR spectroscopy, *J. Atmos. Chem.*, *2*, 191–202, 1984.

Mihelcic, D., D. H. Ehhalt, G. F. Kulessa, J. Klomfass, M. Trainer, U. Schmidt, and H. Rohrs, Measurements of free radicals in the atmosphere by matrix isolation and electron paramagnetic resonance, *P. Appl. Geophys.*, *116*, 530–536, 1978.

Stimpfle, R. M., L. B. Lapson, P. O. Wennberg, and J. G. Anderson, Balloon borne in-situ detection of OH in the stratosphere from 37 to 23 kM, *Geophys. Res. Lett.*, *16*, 1433–1436, 1989.

Stimpfle, R. M. and J. G. Anderson, In-situ detection of OH in the lower stratosphere with a balloon borne high repetition rate laser system, *Geophys. Res. Lett.*, *15*, 503–1506, 1988.

Traub, W. A., D. G. Johnson, and K. V. Chance, Stratospheric hydroperoxyl measurements, *Science*, *247*, 446–449, 1990.

Wennberg, P. O., R. M. Stimpfle, E. M. Weinstock, A. E. Dessler, S. A. Lloyd, L. B. Lapson, J. J. Schwab, and J. G. Anderson, Simultaneous, in situ measurements of OH, HO_2, O_3, and H_2O: A test of modeled stratospheric HO_x chemistry, *Geophys. Res. Lett.*, this issue, 1990.

WMO, *Atmospheric Ozone 1985*, Global ozone research and monitoring project, Report No. 16, Geneva, Switz., 1986.

J. Anderson, L. Lapson, R. Stimpfle and P. Wennberg, Harvard University, ESL, 40 Oxford St., Cambridge, MA 02138.

(Recieved July 12, 1990;
accepted August 6,1990)